


Heat current magnification in classical and quantum spin networks

Vipul Upadhyay^{1,*}, Poshika Gandhi², Rohit Juneja¹ and Rahul Marathe^{1,†}

¹*Department of Physics, Indian Institute of Technology Delhi, Hauz Khas 110 016, India*

²*Institute of Physics, University of Freiburg, Hermann-Herder-Str. 3, 79104 Freiburg, Germany*

 (Received 19 October 2022; revised 10 February 2023; accepted 28 February 2023; published 14 March 2023)

We investigate heat current magnification (CM) due to asymmetry in the number of spins in two-branched classical as well as quantum spin systems that are kept between two heat baths at different temperatures. We study the classical Ising-like spin models using Q2R and Creutz cellular automaton dynamics. We show that just the difference in the number of spins is not enough and some other source of asymmetry like unequal spin-spin interaction strengths in the upper and lower branches is required for heat CM. We also provide a suitable physical motivation for CM along with ways to control and manipulate it. We then extend this study to a quantum system with modified Heisenberg XXZ interaction and preserved magnetization. Interestingly, in this case, just the asymmetry in the number of spins in the branches is enough to achieve heat CM. We observe that the onset of CM is accompanied by a dip in the total heat current flowing through the system. We then discuss how the observed CM characteristics can be attributed to the intersection of nondegenerate energy levels, population inversion, and atypical magnetization trends as a function of the asymmetry parameter in the Heisenberg XXZ Hamiltonian. Finally we use the concept of ergotropy to support our findings.

DOI: [10.1103/PhysRevE.107.034120](https://doi.org/10.1103/PhysRevE.107.034120)

I. INTRODUCTION

Heat currents can influence systems in a significant manner at the nanoscale and, as a result, their control and manipulation at small scale is currently a subject of intense research in both the classical as well as quantum domain. These studies may be broadly divided into two categories, one dealing with finding ways to control heat currents by modeling and manufacturing small-scale thermal devices like thermal diodes [1–10], thermal transistors [11–19], etc., and the other more direct way of explicitly studying heat current transport and distribution in various systems, and developing transportation theories [20–30]. Interestingly, for a multibranched system kept between two heat baths at different temperatures, it is observed that under certain conditions heat current in one of the branches may become larger than the total current flowing between the baths, thus leading to the phenomenon called the current magnification (CM) or circular current [25,31–40]. CM has been shown to exist in a wide variety of physical systems like spins [31], molecules [34,39], classical harmonic chains [35,40], and metallic rings [33,41]. In general, it is observed that to get CM, the system must possess either rotational or reflection asymmetry [31]. For the simplest case of a system containing two branches, the heat current can flow in three possible ways, namely, parallel currents in the branches, clockwise circulating current, and anticlockwise circulating current (see Fig. 1). In a recent study [31], it was observed that it is possible to get circulating heat currents in quantum spin systems with modified Heisenberg exchange interactions if the on-site magnetic field is inhomogeneous and the total

magnetization of the system is conserved. However, it is difficult to realize this system experimentally as applying different magnetic fields at different sites for such small systems is in general a difficult task. Motivated by this and earlier studies on heat CM, here we study some simple classical and quantum models for heat CM in two-branched spin systems. In particular, we study the heat current flow in the classical Creutz cellular automaton (CCA) and Q2R models described in Refs. [42–46]. We consider systems with unequal branch spin numbers and with equal as well as unequal branch spin-spin interaction strengths. We find the required conditions for getting CM and the range of parameters that optimize it. We also study a five-spin quantum system similar to Ref. [31] but with spin-number asymmetry in two branches. We use the Redfield master equation and explore the heat flow and energetics in it. Similar to the classical models, we find the parameter range suitable for getting CM in this system. The models that are studied in this paper can have possible experimental realizations, for example, in systems like quasi-1D Ising chains [47,48] or quantum simulators like NMR [49,50], quantum dots [51,52], and trapped ions [53,54].

The paper is organized as follows. In Sec. II, we consider the classical spin models and provide analytical and numerical results. In Sec. III, we discuss the numerical [55] implemen-

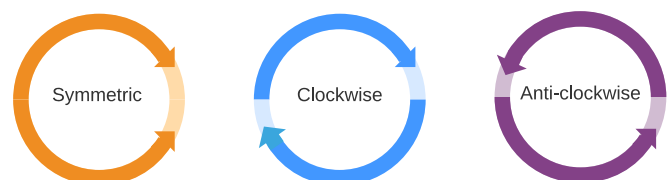


FIG. 1. Possible ways for current to flow in a two-branch system (motivated from Ref. [31]).

*vipupadhyay4@gmail.com

†maratherahul@physics.iitd.ac.in

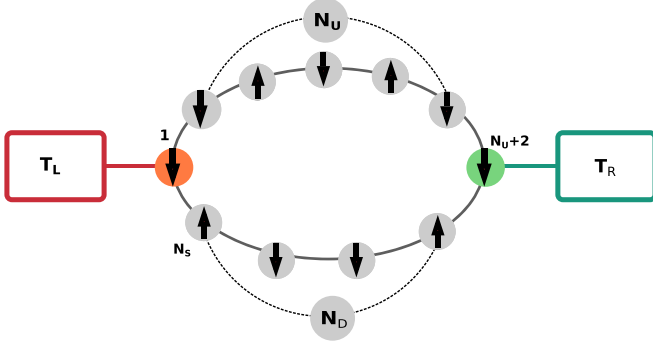


FIG. 2. Schematic representation of the model system.

tation of branch spin number asymmetry in the quantum case by analyzing our system by the Redfield master equation and highlight the relative ease for achieving CM in our model. We summarize our findings and conclude in Sec. IV.

II. MODEL AND CLASSICAL ANALYSIS

We consider an Ising-like two-state spin chain with periodic boundary conditions as shown in Fig. 2. This system is kept between two heat baths at temperatures T_L and T_R to its left and right, respectively. The system interacts with the heat baths at two individual nodes such that only the nodal spins are in direct contact with them while the bulk spins are not. This results in the formation of two spin branches between the baths as shown in Fig. 2. We use N_U (N_D) for the number of spins in the upper (lower) branch which are not in contact with the heat baths. So the total number of spins is given by $N_S = N_U + N_D + 2$. The spins are numbered in clockwise direction, i.e., starting from the spin in contact with the left bath followed by the upper branch spins and then the lower branch spins implying that the spins numbered 1 and $N_U + 2$ interact with the left and right baths, respectively. The state or configuration of our system is described as

$$\eta = \{\sigma_1, \sigma_2, \dots, \sigma_{N_U+2}, \dots, \sigma_{N_S}\}, \quad (1)$$

where σ_i denotes the state of i th spin and $\sigma_i \in \{-1, 1\}$. The energy corresponding to a particular configuration is decided by the Hamiltonian of the system. For the cases that we study in this paper, only the nearest-neighbor spin-spin interaction are considered. Thus, the Hamiltonian is given by

$$H_S^I = - \sum_i J_i \sigma_i \sigma_{i+1}, \quad (2)$$

where H_S^I is the spin-spin interaction term in the total Hamiltonian, J_i is the interaction strength between the i th and $(i+1)$ th spin and $\sigma_{N_S+1} = \sigma_1$. This means that the energy cost for flipping a spin σ_i is

$$\Delta E_i = 2J_i \sigma_i \sigma_{i+1} + 2J_{i-1} \sigma_i \sigma_{i-1}, \quad (3)$$

subject to the periodic boundary conditions. Due to the interaction with the baths as well as the internal interaction between the spins, the configuration of the system may change, resulting in the flow of heat currents in our system.

A. Time evolution dynamics

To carry our analysis forward, we first need to define the appropriate time evolution dynamics for our system. The master equation for our system is characterized by configuration pairs (η, η^i) where η^i is same as η except for the flip of i th spin and is given as

$$\frac{dP(\eta)}{dt} = \sum_{i=1}^{N_S} r_{\eta^i \rightarrow \eta} P(\eta^i) - \sum_{i=1}^{N_S} r_{\eta \rightarrow \eta^i} P(\eta), \quad (4)$$

where $P(\eta)$ is the probability of finding the system in the configuration η at time t and $r_{\eta^i \rightarrow \eta}$ is the transition rate for flipping spin i and taking the system from configuration η^i to η . As already discussed above, for our model the nodal spins are in direct contact with the baths while the bulk spins are not. This suggests that to study our system, we need hybrid dynamics with separate transition rates for nodal and bulk spins.

First, because of their interaction with the baths, the dynamics of the nodal spins can be studied using the Metropolis algorithm, for which a spin flips according to the following transition rate [1]:

$$r_{\eta \rightarrow \eta^i}^\alpha = \min(1, e^{-\beta_\alpha \Delta E_i}), \quad (5)$$

where $\beta_\alpha = 1/k_B T_\alpha$, $\alpha \in \{L, R\}$, $i \in \{1, N_U + 2\}$ and we work in units where $k_B = 1$. Since the bulk spins are not in contact with any baths, a dynamics involving random numbers is not suitable for them and a deterministic energy-conserving dynamics is needed for understanding their time evolution. Such kinds of dynamics generally fall under cellular automaton [42,56]. We use two different types of cellular automaton for our problem: first, the Q2R dynamics in Sec. IID and then the CCA dynamics in Sec. IIG. We now discuss the current definitions required for the classical analysis.

B. Heat current definitions

To define the heat current flowing out of a bath, we look at the nodal spin associated with it and identify all the configuration pairs (η, η^i) which differ by its flip. The corresponding heat energy flow is then given as

$$I_\alpha = \sum_{(\eta, \eta^i)} \Delta E_i (r_{\eta \rightarrow \eta^i}^\alpha P(\eta) - r_{\eta^i \rightarrow \eta}^\alpha P(\eta^i)), \quad (6)$$

where the sum runs over all the configuration pairs that differ by a flip of the i th spin with $\alpha \in \{L, R\}$ for $i \in \{1, N_U + 2\}$. Since the bulk spins are not in contact with the baths, their flipping should cause no change in total energy of the system for any of the dynamics used. As a result, Eq. (6) gives us zero when applied for flipping of bulk spins. However, the flip of bulk spins still leads to a transfer of energy from one spin to other over a bond [43]. To better understand this, let us consider the interaction energy associated with a spin i :

$$E_i = -J_i \sigma_i \sigma_{i+1} - J_{i-1} \sigma_i \sigma_{i-1}. \quad (7)$$

The above expression contains the two bond energy terms associated with spin i . Since this spin does not interact with the baths, it can flip only when the associated energy cost given in Eq. (3) is either zero or can be compensated by some other noninteracting internal energy of the system. In

both cases, the individual bond energies change, signifying a transfer of energy through the bonds and hence a heat current. Focusing on the $i-i+1$ bond, the energy transferred through it on the flipping of the i th spin is

$$\Delta E_{i,i+1} = 2J_i\sigma_i\sigma_{i+1}. \quad (8)$$

To find the associated heat current, we identify all the configuration pair transitions related by the flip of the i th spin but focus only on the corresponding energy change on the $i-i+1$ bond. This gives the following expression for heat current passing through bulk spin i :

$$I_{U(D)} = \sum_{(\eta,\eta^i)} \Delta E_{i,i+1}(r_{\eta\rightarrow\eta^i}P(\eta) - r_{\eta^i\rightarrow\eta}P(\eta^i)), \quad (9)$$

where $I_{U(D)}$ is the heat current in the upper (lower) branch depending on the position of the i th spin. Since the flipping of the bulk spins is deterministic, it will either definitely happen or is completely forbidden and, as a result, $r_{\eta\rightarrow\eta^i} \in \{0, 1\}$, unlike the stochastic flipping of the nodal spins. Finally, CM occurs when the heat current in one of the branches is larger than the current flowing between the system and the bath. According to the convention used in the current definitions above, we get CM if both branch currents have the same sign.

C. Information about methodology

We now discuss the methodology [57] used to find results for the classical case. All the results shown in this paper are for the steady state. The simulations for the classical case are performed by randomly selecting a spin and flipping it depending on a suitable dynamics. Here, we use a hybrid dynamics involving the metropolis algorithm for the nodal spins and the Q2R or CCA dynamics for the bulk spins. Whichever the case, only one spin is allowed to flip per time step. The system is allowed to relax to the steady state and the required quantities are then calculated. The corresponding numerical and analytical calculations are done by writing the master equation and solving the transition matrix like the one given in Eq. (11). Since we are only interested in the steady state calculations, we require the eigenvector corresponding to the eigenvalue 0 of the transition matrix. On applying the probability normalization condition on this eigenvector,

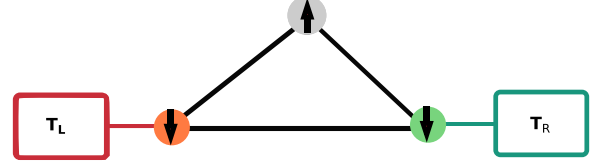


FIG. 3. Illustration of the model system consisting of three spins with $N_U = 1$ and $N_D = 0$.

steady-state probabilities can be obtained. These can then be used to calculate the currents analytically.

Note on experimental parameter range. In the units that we work in, for both classical and quantum systems, the effect on the system due to the interaction with the baths is quantified by an expression of the type $e^{J/T}$. This means that for any meaningful dynamics to take place, the temperature of the baths should correspond to the thermal energy of the same order as J . The value of J is typically decided by the experimental setup being studied. For example, in the experimental setup studied by Coldea *et al.* [47], the value of J is in few meV, which roughly corresponds to the thermal energy associated with temperatures of order 10 K.

D. Q2R dynamics with symmetric upper and lower branch interaction strength

We start our analysis by studying the Q2R dynamics [43,44] for the flipping of the bulk spins. This is one of the simplest models which allows us to have a deterministic mechanism for time evolution of the bulk spins while preserving the total energy of the system. The Hamiltonian for this model is the same as the typical Ising Hamiltonian and is obtained by substituting $J_i = J$ in Eq. (2). According to this dynamics, a bulk spin i can flip only if its neighboring spins have opposite orientations, i.e.,

$$\sigma_{i-1} = -\sigma_{i+1}. \quad (10)$$

This ensures us that the total energy change of the system in Eq. (3) is zero on flipping of the bulk spin. To better understand the implications of the Q2R dynamics, we perform an analytical study for the minimalistic model with just three spins and $N_U = 1$ and $N_D = 0$ as shown in Fig. 3. This being the simplest case, where the required asymmetric spin branching is possible, it offers a good starting point. The master equation (4) for this system written in the matrix form is given by

$$\frac{d}{dt} \begin{pmatrix} P(\downarrow, \downarrow, \downarrow) \\ P(\uparrow, \downarrow, \downarrow) \\ P(\downarrow, \uparrow, \downarrow) \\ P(\uparrow, \uparrow, \downarrow) \\ P(\downarrow, \downarrow, \uparrow) \\ P(\uparrow, \downarrow, \uparrow) \\ P(\downarrow, \uparrow, \uparrow) \\ P(\uparrow, \uparrow, \uparrow) \end{pmatrix} = \begin{pmatrix} -e^{-4J\beta_L} - e^{-4J\beta_R} & 1 & 0 & 0 & 1 & 0 & 0 & 0 \\ e^{-4J\beta_L} & -3 & 0 & 1 & 0 & 1 & 0 & 0 \\ 0 & 0 & -2 & 1 & 0 & 0 & 1 & 0 \\ 0 & 1 & 1 & -3 & 0 & 0 & 0 & e^{-4J\beta_R} \\ e^{-4J\beta_R} & 0 & 0 & 0 & -3 & 1 & 1 & 0 \\ 0 & 1 & 0 & 0 & 1 & -2 & 0 & 0 \\ 0 & 0 & 1 & 0 & 1 & 0 & -3 & e^{-4J\beta_L} \\ 0 & 0 & 0 & 1 & 0 & 0 & 1 & -e^{-4J\beta_L} - e^{-4J\beta_R} \end{pmatrix} \begin{pmatrix} P(\downarrow, \downarrow, \downarrow) \\ P(\uparrow, \downarrow, \downarrow) \\ P(\downarrow, \uparrow, \downarrow) \\ P(\uparrow, \uparrow, \downarrow) \\ P(\downarrow, \downarrow, \uparrow) \\ P(\uparrow, \downarrow, \uparrow) \\ P(\downarrow, \uparrow, \uparrow) \\ P(\uparrow, \uparrow, \uparrow) \end{pmatrix}. \quad (11)$$

Solving the master equation (as discussed in Sec. II C), we arrive at the following steady state probabilities:

$$\begin{aligned}
 P(\downarrow, \downarrow, \downarrow) &= \frac{e^{4J\beta_L + 4J\beta_R}}{\mathcal{D}_1}, & P(\uparrow, \downarrow, \downarrow) &= \frac{3e^{4J\beta_L} + 5e^{4J\beta_R}}{8\mathcal{D}_1}, \\
 P(\downarrow, \uparrow, \downarrow) &= \frac{e^{4J\beta_L} + e^{4J\beta_R}}{2\mathcal{D}_1}, & P(\uparrow, \uparrow, \downarrow) &= \frac{5e^{4J\beta_L} + 3e^{4J\beta_R}}{8\mathcal{D}_1}, \\
 P(\downarrow, \downarrow, \uparrow) &= \frac{5e^{4J\beta_L} + 3e^{4J\beta_R}}{8\mathcal{D}_1}, & P(\uparrow, \downarrow, \uparrow) &= \frac{e^{4J\beta_L} + e^{4J\beta_R}}{2\mathcal{D}_1}, \\
 P(\downarrow, \uparrow, \uparrow) &= \frac{3e^{4J\beta_L} + 5e^{4J\beta_R}}{8\mathcal{D}_1}, & P(\uparrow, \uparrow, \uparrow) &= \frac{e^{4J\beta_L + 4J\beta_R}}{\mathcal{D}_1}.
 \end{aligned} \tag{12}$$

where

$$\begin{aligned}
 \mathcal{D}_1 &= 2e^{2J(\beta_R + \beta_L)}\mathcal{D}, \text{ with } \mathcal{D} \\
 &= (3 \cosh(2J(\beta_R - \beta_L)) + e^{2J(\beta_L + \beta_R)}),
 \end{aligned} \tag{13}$$

and the notation $P(\uparrow, \downarrow, \downarrow)$ specifies the probability of getting the left spin up, middle spin down, and right spin down, respectively. Using the above probabilities and the rates defined in Eq. (5), the steady-state heat current flowing out of the left bath in Eq. (6) becomes

$$\begin{aligned}
 I_L &= \frac{8}{3}J(e^{-4J\beta_L}P(\downarrow, \downarrow, \downarrow) - P(\uparrow, \downarrow, \downarrow)) \\
 &= J \sinh(2J(\beta_R - \beta_L))/\mathcal{D}.
 \end{aligned} \tag{14}$$

Similarly, the branch heat currents are found by using Eq. (9) for the bulk spins in the upper and lower branches and have the following expressions:

$$\begin{aligned}
 I_U &= \frac{J}{3} \sinh(2J(\beta_R - \beta_L))/\mathcal{D}, \\
 I_D &= -\frac{2J}{3} \sinh(2J(\beta_R - \beta_L))/\mathcal{D}.
 \end{aligned} \tag{15}$$

From the above expressions for total and branch currents, we see that all currents go to zero for equal temperatures of baths as expected. For different bath temperatures, the branch currents add up to give us the total current, i.e., $I_L = I_U - I_D$. The minus sign comes because of the convention used for defining the current direction in the system (+ve when current direction is left to right). Also, the magnitude of the total current is always greater than the magnitude of the branch currents for any values of system parameters, so heat CM is not possible for this system. Interestingly, the heat current flowing through a branch is inversely proportional to the number of spin-spin bonds in that branch. This is similar to Ohm's law in an electric circuit with the spin-spin bond behaving analogous to a resistor. The corresponding simulation results for this model are shown in Fig. 4. We see in Fig. 4(a) that for the three-spin system, our analytical and numerical results match perfectly with the simulation results. In Fig. 4(b), we plot the current as a function of the temperature of the left bath T_L , keeping the temperature of right bath T_R fixed. We find that the heat currents are nonmonotonic functions of temperature difference, initially increasing sharply and then saturating for a large temperature difference between the baths. To understand why this is so, we put the limit of large temperature gradient $T_L \gg T_R$ in Eqs. (13)–(15). Since we have fixed $T_R = 1$, this

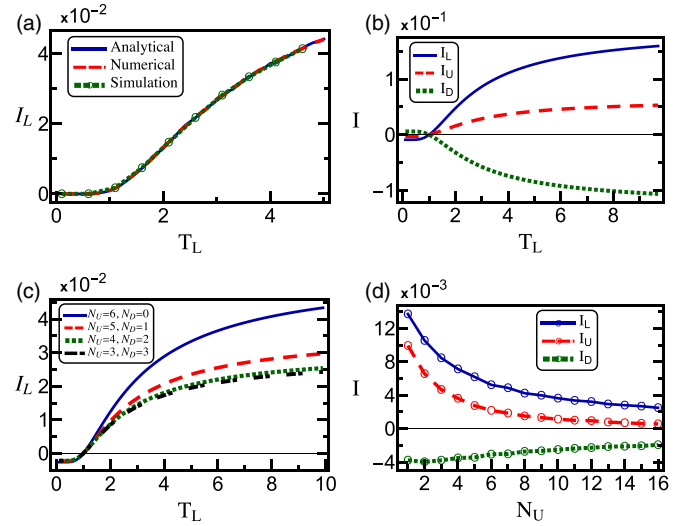


FIG. 4. (a) Comparison of total current (I_L) between analytical, numerical, and simulation results for the three-spin system with $N_U = 1$, $N_D = 0$, (b) variation of heat currents (I) with T_L for $N_U = 1$, $N_D = 0$, (c) variation of I_L with T_L for an eight-spin system but with different branch spin distributions, (d) variation of heat currents (I) with N_U for $N_D = 4$, $T_L = 2$, $T_R = 0.1$. For all cases unless otherwise specified, we use $T_R = 1$, $J = 1$.

means that $T_L \gg 1$ and $\beta_R \pm \beta_L \sim \beta_R$. Using this, we get the following asymptotic expressions for currents:

$$\begin{aligned}
 I_L &\sim \frac{J \sinh(2J\beta_R)}{3 \cosh(2J\beta_R) + e^{2J\beta_R}}, \\
 I_U &\sim \frac{\frac{J}{3} \sinh(2J\beta_R)}{3 \cosh(2J\beta_R) + e^{2J\beta_R}}, & I_D &\sim \frac{\frac{-2J}{3} \sinh(2J\beta_R)}{3 \cosh(2J\beta_R) + e^{2J\beta_R}}.
 \end{aligned} \tag{16}$$

We see that the above expressions are independent of $\beta_L(T_L)$, hence the current saturates for large values of T_L . We also note from Fig. 4(c) that the total current flowing in the system does not only depend upon the total number of spins but also on how they are distributed in branches. In Fig. 4(d), we see that the current decreases with an increase in the number of spins which is consistent with our earlier proposition of the spin-spin bonds behaving similarly to the resistors. From the above analysis, it is clear that we will not get CM just by branch spin number asymmetry for the Q2R dynamics, and a dynamics with additional source of asymmetry is required. We study one such dynamics in the next section.

E. Q2R dynamics with asymmetric upper and lower branch interaction strength

Since just the branch spin number asymmetry is not sufficient for generating CM, we now employ different spin-spin interaction strengths in the upper and lower spin branches as a new source of asymmetry in our model. This effectively means that we have two different thermal wires for upper and lower branches. The Hamiltonian for this system is given as

$$H_S = -J_1 \sum_{i=1}^{N_U+1} \sigma_i \sigma_{i+1} - J_2 \sum_{i=N_U+2}^{N_S} \sigma_i \sigma_{i+1}. \tag{17}$$

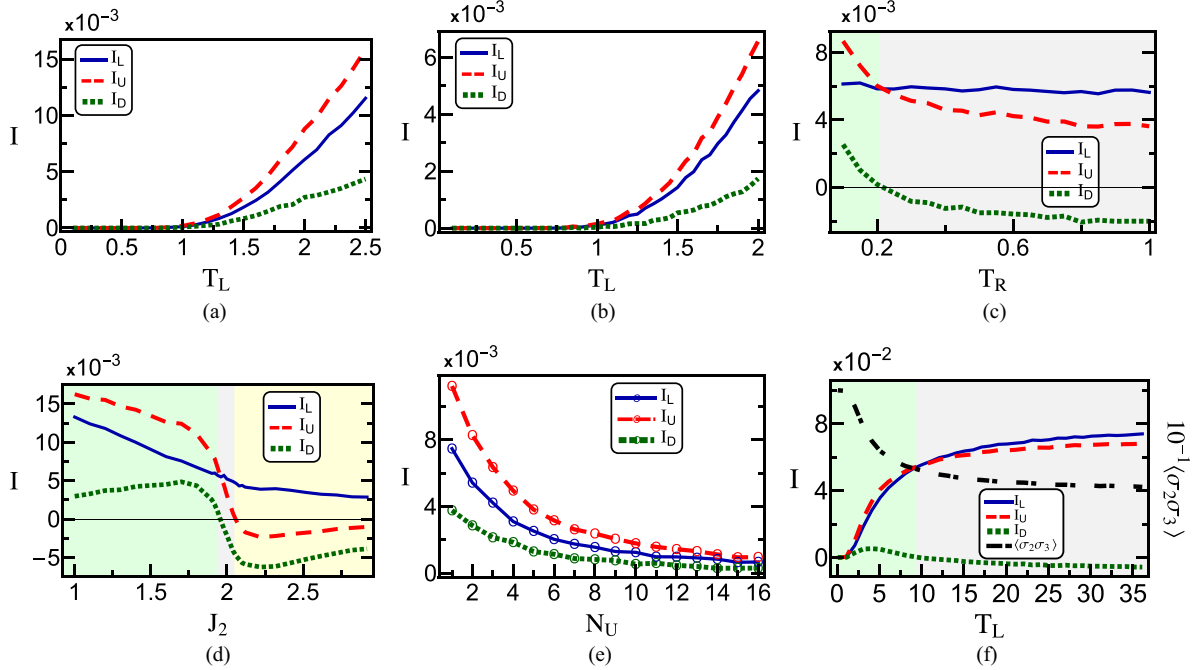


FIG. 5. Variation of heat currents (I) with (a) T_L , with (b) T_L for $N_D = 2, N_U = 3$, with (c) T_R , with (d) J_2 , with (e) N_U for $N_D = 4$, and (f) variation of heat currents (I) and $\langle \sigma_2 \sigma_3 \rangle$ with T_L . For all cases, unless otherwise specified we use $J_1 = 2, T_L = 2, T_R = 0.1, J_2 = 1.9, N_D = 3, N_U = 2$. In all figures where multiple regions of current circulation directions are present, we use green, gray, and yellow background colors to indicate clockwise, parallel, and anticlockwise circulating currents, respectively. For all other cases, we use a white background.

Similar to the previous case, it is possible to analytically solve this model for a three-spin system but the expressions are too complicated to be included here. However, we can still infer the general characteristic of this model by looking at the simulation results given in Fig. 5. We see in Fig. 5(a) that it is possible to get CM for asymmetric branch interaction strengths in the Q2R model if the system parameters are in optimal range. This deviates from our earlier observations and tells us that for different interaction strengths in upper and lower branches, we can no longer assume the bond as being analogues to a resistor. In Fig. 5(b), we see that interchanging the number of spins in the branches still gives us current circulation in the same direction but the magnitudes of currents change. We also note [see Fig. 5(c)] that we need the temperature of one of the heat baths to be an order below the energy scale of the bond interaction energy to achieve significant CM. Interestingly, as seen Fig. 5(d), increasing the difference between interaction strengths of the branches does not necessarily increase the relative CM and a possibility for optimization of CM exists. We see that the direction of current circulation changes depending on the relative magnitude of interaction strength in upper and lower branches. This may result in a scenario where no current flows through one spin branch and total current equals one of the branch currents. This happens for $J_2 \sim 2$ in Fig. 5(d). We also see in Fig. 5(e) that the magnitudes of the currents decrease with an increase in the number of spins and CM is possible even for the same number of spins in the branches. To check how the CM depends on the spin-spin correlation defined as

$$\langle \sigma_i \sigma_j \rangle = \sum_{\{\sigma\}} P(\{\sigma\}) \sigma_i \sigma_j, \tag{18}$$

where the sum runs over all the system configurations $\{\sigma\}$ and $P(\sigma)$ is the probability of getting a particular configuration σ . We plot the currents as well as the correlation between spins 2 and 3, namely, $\langle \sigma_2 \sigma_3 \rangle$ in Fig. 5(f) and see that for the region where we get CM, the spin-spin correlation is high and when it decreases the magnification also decreases. We now discuss a possible physical mechanism behind this.

F. Possible physical mechanism

To make sense of the results observed above, we study the example of an energy transfer process in a four-spin system with ' $N_U = 1, N_D = 1$ ' as shown in Fig. 6. The configuration change steps corresponding to this process are

$$\{\uparrow\uparrow\uparrow\downarrow\} \rightarrow \{\downarrow\uparrow\uparrow\downarrow\} \rightarrow \{\downarrow\downarrow\uparrow\downarrow\} \rightarrow \{\downarrow\downarrow\uparrow\uparrow\} \rightarrow \{\downarrow\downarrow\downarrow\uparrow\}, \tag{19}$$

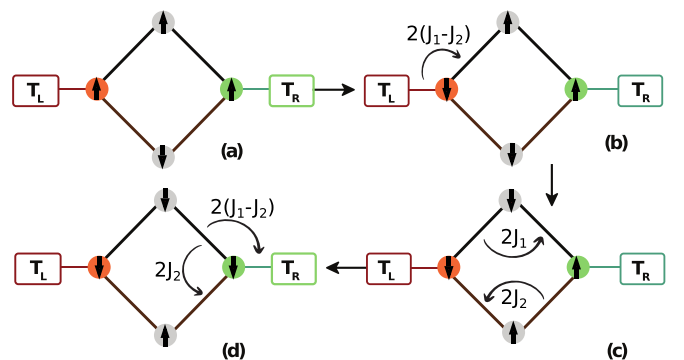


FIG. 6. Example of a process which results in the transfer of energy $2(J_1 - J_2)$ from left bath to right bath.

where, as before, the arrows indicate the states of spins numbered from left to right. The spins numbered 1 and 3 interact with the left and right baths, respectively, and follow Metropolis dynamics while spins 2 and 4 follow Q2R dynamics. The bond interaction strength is J_1 and J_2 for upper and lower spin branches, respectively. The first step in the process involves the flipping of the first spin via the Metropolis algorithm and signifies a transfer of energy $2(J_1 - J_2)$ from the left bath to the system [see Fig. 6(a)]. The next two steps in the process are shown in Fig. 6(b) and involve the deterministic flipping of the bulk spins via the Q2R dynamics that result in energy transfer of magnitude $2J_1$ in the upper branch and $-2J_2$ in the lower branch successively. The final step involves the flipping of the right nodal spin, which indicates an energy transfer of magnitude $2(J_1 - J_2)$ from the upper system branch to the right bath and simultaneously a energy transfer of $2J_2$ from the upper branch to the lower branch [see Fig. 6(d)]. Looking at the cumulative effect of all these steps, we get a process resulting in transfer of energy $2(J_1 - J_2)$ from the left bath to the right bath accompanied by the flow of $2J_1$ energy in the upper branch and $2J_2$ energy in the lower branch, hence resulting in CM and clockwise current circulation inside the system. For the circulation of the same energy in the anticlockwise direction, we will have to transfer the energy $2(J_1 - J_2)$ from the right bath to the left bath, which has less probability because of the lower temperature of the right bath, hence this process gives us a net current circulation.

The other way to transfer energy from the left to right bath includes a process where the energy transfer is of magnitude $2(J_1 + J_2)$. This gives us no current circulation, but since the energy is of higher magnitude this process has less probability of occurrence. Thus, overall, the process with current circulation dominates the energy transfer and hence CM happens on an average. But if the temperature of right bath is increased, the probability of the reverse process also increases and current circulation decreases, as seen in Fig. 5(b). Increasing the gap between values of J_1 and J_2 increases the energy transfer magnitude $2(J_1 - J_2)$, making the process less and less probabilistic, hence reducing relative CM. Therefore, large CM is achieved if the interaction strengths are of a similar order of magnitude [see Fig. 5(c)]. The above mechanism also explains why we will not get any heat current for symmetric interaction strength in both branches as the net current due to this process becomes zero. No such heat transfer process is possible when we have the two nodal spins directly connected to each other, so there will be no CM in such a case as well. The corresponding simulation results for the system shown in Fig. 6 are shown in Fig. 7. We see qualitatively similar results for this case as in Fig. 5, though the value of the circulating current is small pertaining to the symmetry in the number of spins in the upper and lower branch.

G. CCA model

In the Q2R dynamics discussed above, the system Hamiltonian consisted of only the interaction energy terms and as such the heat current in the bulk could only be transferred through the passing of energy from one bond to the other. We now work with a model which allows additional ways for the system to possess energy. To achieve this, we use the

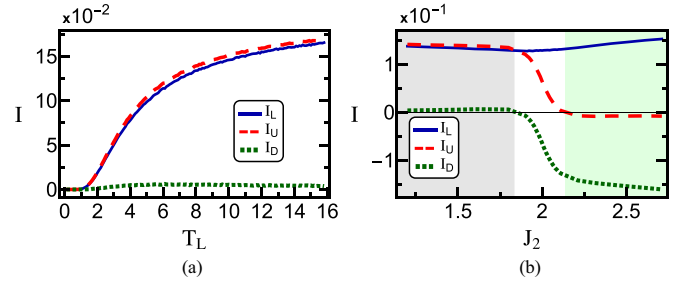


FIG. 7. Variation of Heat Currents (I) with (a) T_L , with (b) J_2 for the system shown in Fig. 6 with $N_D = 1, N_U = 1$. For all the cases, unless otherwise specified we use $J_1 = 2, T_L = 2, T_R = 0.1, J_2 = 1.9$.

relatively complex CCA dynamics [43,44] for studying the time evolution of bulk spins. This dynamics allows for a change in interaction energy of the system by using an additional source of energy at each site, a local “demon” [44]. As stated earlier, for studying this dynamics we need to modify the total Hamiltonian and include an extra energy term to each spin site. This term corresponds to the presence of kinetic energy at each site and this results in the following total Hamiltonian:

$$H_S = -J_1 \sum_{i=1}^{N_U+1} \sigma_i \sigma_{i+1} - J_2 \sum_{i=N_U+2}^{N_S} \sigma_i \sigma_{i+1} + \mu \sum_{i=1}^{i=N_S} \tilde{\sigma}_i, \quad (20)$$

where μ is the scaling parameter for the kinetic energy reserve at each site and $\tilde{\sigma}_i$ represents the state of this new degree of freedom with $\tilde{\sigma}_i \in \{0, 1, 2, 3\}$. The presence of additional energy reserves at each site leads to the possibility of more bulk spins flips as some of the extra energy changes can be compensated. Since the magnitude of energy supplied by the kinetic energy reserve is in multiples of μ , the bulk spin i can only flip under this dynamics if the following condition is satisfied:

$$\mu \tilde{\sigma}_i - \Delta E_i \in \{0, \mu, 2\mu, 3\mu\}, \quad (21)$$

where, $\Delta E_i = 2J_i \sigma_i (\sigma_{i-1} + \sigma_{i+1})$ and it can take the values $\Delta E_U \in \{0, \pm 4J_1\}$ or $\Delta E_D \in \{0, \pm 4J_2\}$ for upper and lower branch spins, respectively. The above equation tells us that the bulk spin i can only flip if its kinetic energy reserve can compensate for the corresponding energy cost. So, the dynamics is still deterministic and total energy is conserved for the flip of a bulk spin. A consequence of the above condition is that for CCA to allow additional flips than Q2R, the values μ and J_1, J_2 must be related. To illustrate this, we give a few particular examples. If we choose $J_1 = 2, J_2 = 1$, and $\mu = 4$, then CCA dynamics can be applied for both branches. Since, for $\mu = 4, \mu \tilde{\sigma} \in \{0, 4, 8, 12\}$, $|\Delta E_U| \in \{0, 8\}$, and $|\Delta E_D| \in \{0, 4\}$. However, for some other value, say, $\mu = 2$, we have $\mu \tilde{\sigma} \in \{0, 2, 4, 6\}$, $|\Delta E_U| \in \{0, 8\}$, and $|\Delta E_D| \in \{0, 4\}$. Hence, for the upper branch, we essentially have the Q2R dynamics because the condition in Eq. (21) is only satisfied for $\Delta E_U = 0$, but for the lower branch CCA dynamics still applies. We can see that irrespective of the particular values of J_1, J_2 , and μ , the above condition is always satisfied for zero energy change and the Q2R dynamics always remains embedded in the CCA dynamics. Since the interaction energy of the spin bonds still remains the same, flipping of a spin signifies the

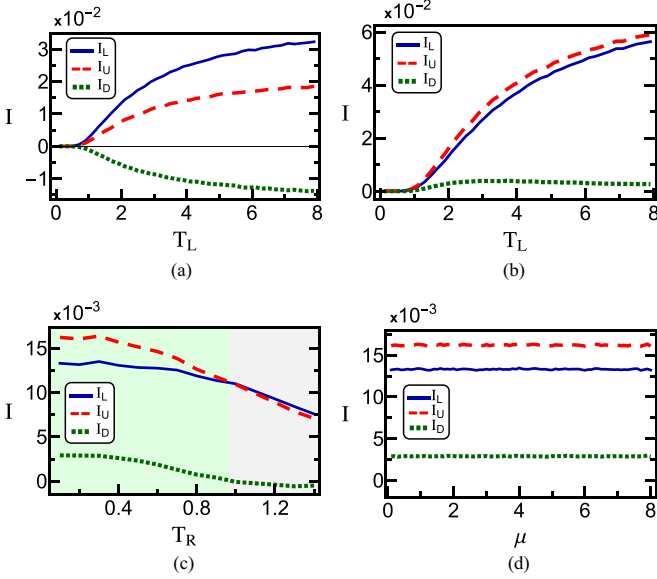


FIG. 8. Variation of Heat Currents (I) for the CCA model with (a) T_L for $J_1 = J_2 = 1$, with (b) T_L , with (c) T_R and (d) with μ . For all the cases unless otherwise specified $J_1 = 2$, $T_L = 2$, $T_R = 0.1$, $J_2 = 1$, $N_D = 3$, $N_U = 2$, and $\mu = 4$.

same transfer of energy as before but that energy could come either from the neighboring bond or the kinetic energy reserve. The expressions for heat currents remain the same and are still given by Eqs. (6) and (9). Simulating this model gives us the results shown in Fig. 8.

In Fig. 8(a), we see that it is not possible to get CM even in the CCA model just by the branch spin number asymmetry and the total heat current distribution still has Ohm's law like characteristics for symmetric upper and lower branch interaction strengths. Similar to the earlier cases, we see in Fig. 8(b) that we can get CM for this model if the spin-spin interaction strength differs in upper and lower branches. In Fig. 8(c), we see that the CM is possible only when the temperature of one of the baths is an order below the interaction energy of the bonds. Finally, on studying the variation of current with μ in Fig. 8(d), we see that the steady-state currents are independent of the values of μ , even though CCA dynamics allows additional flips when $\mu \in \{2, 4, 8\}$. This means that we get similar steady-state heat currents for both CCA and Q2R models for similar values of system parameters. The extra momentum term does not contribute critically to the steady-state heat currents. This is in agreement with what was observed by Saito *et al.* [43].

III. QUANTUM ANALYSIS

We now want to study the effects of branch spin number asymmetry on the heat current transport in the quantum domain. To do this, we perform a complementary study to the one performed by Xu *et al.* [31]. It was shown by them that it is possible to get heat CM in a quantum system with four spins interacting via modified Heisenberg exchange interaction if the on-site magnetic field is inhomogeneous and the total magnetization of the system is conserved. However, it is difficult to realize this system experimentally as

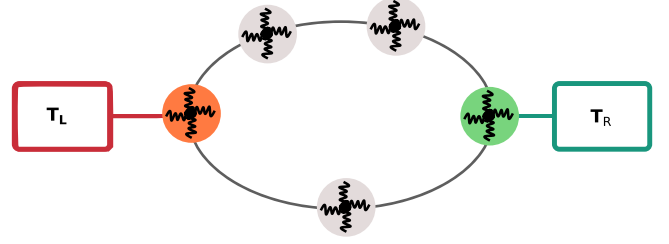


FIG. 9. Illustration of the quantum spin system consisting of five spins with $N_U = 2$ and $N_D = 1$.

applying different magnetic fields at different sites for such small systems is, in general, a difficult task. So, in place of the inhomogeneous magnetic field, we use unequal number of spins in branches similar to the classical models. This will also help us to distinguish the CM in quantum spin systems from the classical ones.

A. The model

We study a five-spin quantum system containing unequal branch spin numbers as shown in Fig. 9. The spins are interacting with each other via a slightly modified Heisenberg XXZ interaction [31] and the system Hamiltonian is given as

$$\hat{H}_S = J \sum_i (\hat{\sigma}_x^i \hat{\sigma}_x^{i+1} + \hat{\sigma}_y^i \hat{\sigma}_y^{i+1}) + \Delta \hat{\sigma}_z^i \hat{\sigma}_z^{i+1}, \quad (22)$$

where J is the interaction strength between the x and y components of neighboring spins, Δ is called the asymmetry parameter of the Heisenberg XXZ interaction and signifies the interaction strength between z components of the spins, $\hat{\sigma}_\alpha^i$ denotes the $\alpha \in \{x, y, z\}$ component of the usual Pauli spin- $\frac{1}{2}$ matrix for the i th spin. The unit operators are denoted by $\hat{1}$ and $\hat{\sigma}_z^i = \frac{\hat{\sigma}_z^{i+1}}{2}$. This slight modification to the usual XXZ interaction is done so the transition to the fermionic system via the Jordan Wigner transformation [58] does not lead to a Δ -dependent local chemical potential [31]. This system is interacting with two Bosonic baths with the following Hamiltonian:

$$\hat{H}_{B_i} = \sum_n \omega_n \hat{a}_n^{\dagger i} \hat{a}_n^i, \quad (23)$$

where $\hat{a}_n^{\dagger i} (\hat{a}_n^i)$ is the creation (destruction) operator of the n th mode of the i th bath. To achieve the spin branch configuration given in Fig. 9, the spins numbered 1 (4) should interact with the left (right) baths, respectively. The system bath interaction is chosen to preserve the initial magnetization of the system and has the form

$$\begin{aligned} \hat{H}_{SB_L} &= \hat{\sigma}_z^1 \otimes \sqrt{\gamma} \sum_n c_n^L (\hat{a}_n^L + \hat{a}_n^{L\dagger}), \\ \hat{H}_{SB_R} &= \hat{\sigma}_z^4 \otimes \sqrt{\gamma} \sum_n c_n^R (\hat{a}_n^R + \hat{a}_n^{R\dagger}), \end{aligned} \quad (24)$$

where $\sqrt{\gamma}$ is the coupling strength between system and the baths and its value is always taken as positive. Though the operator $\hat{\sigma}_z$ can't change the magnetization of a spin, it can still lead to a transfer of energy as the eigenstates of the Hamiltonian and $\hat{\sigma}_z$ are not the same.

B. Master equation

To study the dynamics of the system, we again impose Markovian time evolution and hence the density matrix of our system satisfies a master equation of the type [59],

$$\frac{d}{dt}\hat{\rho}(t) = \mathcal{L}_L\hat{\rho}(t) + \mathcal{L}_R\hat{\rho}(t), \quad (25)$$

where $\hat{\rho}(t)$ is the density matrix of the system of interest at time t and $\mathcal{L}_{L(R)}$ is the Liouvillian operator of the left (right) bath. Specifically, for the analysis in this paper, the Redfield master equation [59,60] is used. This is because the more simpler Lindblad master equation doesn't give the correct coherences in the steady state and hence we obtain incorrect branch currents in that case [31,61]. The Redfield master equation is used for the weak coupling regime between the system and the baths and is correct only up to order γ [59,60]. Its form for our model in the Schrödinger picture and in the energy basis is given as (working in the units where $\hbar = 1$)

$$\begin{aligned} \dot{\rho}_{nm} = & -i\Delta_{nm}\hat{\rho}_{nm} + \gamma \sum_{i,j} \left(\hat{S}_{ni}^L \hat{S}_{jm}^L [\tilde{W}_{jm}^L + W_{ni}^L] \right. \\ & \left. - \delta_{mj} \sum_l \hat{S}_{nl}^L \hat{S}_{li}^L W_{li}^L(0) - \delta_{ni} \sum_l \hat{S}_{jl}^L \hat{S}_{lm}^L \tilde{W}_{jl}^L(0) \right) \rho_{ij} \\ & + \text{right bath terms.} \end{aligned} \quad (26)$$

Here $\hat{\rho}_{nm}$ is the matrix element of the system density matrix and Δ_{nm} is the energy difference between the n th and m th energy levels or $\Delta_{nm} = E_n - E_m$. $\hat{S}^L(\hat{S}^R)$ is the operator of the system that interacts with the left (right) bath and $\hat{S}^{L,R} = \hat{\sigma}_z^{1,4}$ for our case. Finally, the W matrices depend on the system energy spectrum and the heat bath correlations. They are defined as

$$W_{ij}^L = \int_0^\infty dt e^{-i\Delta_{ij}t} C^L(t), \quad \tilde{W}_{ij}^L = \int_0^\infty dt e^{-i\Delta_{ij}t} C^L(-t), \quad (27)$$

with $C^L(t) = Tr_B(\hat{B}_L(t)\hat{B}_L\hat{\rho}_B(0))$, $\hat{B}_L = \sum_n c_n^L(\hat{a}_n + \hat{a}_n^\dagger)$, and $\hat{\rho}_B(0)$ is the equilibrium density matrix corresponding to the bath. Ignoring the Lamb shift terms [59,60], $\tilde{W}_{j,i}^{L(R)} = W_{i,j}^{L(R)}$ and we can write

$$W_{i,j}^{L(R)} = \begin{cases} J(\Delta_{ij})N(\Delta_{ij}, T_{L(R)}) & \Delta_{ij} > 0 \\ J(|\Delta_{ij}|)(1 + N(|\Delta_{ij}|, T_{L(R)})) & \Delta_{ij} < 0, \end{cases} \quad (28)$$

where $N(\omega, T_{L(R)})$ is the Bose-Einstein distribution function,

$$N(\omega, T_{L(R)}) = \frac{1}{e^{\omega/T_{L(R)}} - 1}, \quad (29)$$

and we choose

$$J(\omega) = \omega e^{-\omega/\Omega_C}, \quad (30)$$

as the spectral density of the baths. We fix $\Omega_C = 10$ without loss of generality. Since the above equation is only correct up to the order γ , we take $\sqrt{\gamma} = 0.1$ without loss of generality. The functional form of the bath spectral density and numerical values of Ω_C and γ are similar to the ones taken in Ref. [31].

C. Definitions

We now define the physical quantities required for studying the quantum model. Similar to the classical case, all the results are calculated for the steady state and we denote our steady-state density matrix as

$$\hat{\rho}_S = \lim_{t \rightarrow \infty} \hat{\rho}(t). \quad (31)$$

The expression for the current flowing through a branch is derived by using the Heisenberg equation of motion [59] for the bond energy operator between spins l and $l+1$. The resulting operator for the current flowing through site ' l ' of our system is given as [31]

$$\hat{I}[l] = i[\hat{h}_{l-1,l}, \hat{h}_{l,l+1}], \quad (32)$$

with the bond energy operator inferred from Eq. (22) as

$$\hat{h}_{l,l+1} = J(\hat{\sigma}_x^l \hat{\sigma}_x^{l+1} + \hat{\sigma}_y^l \hat{\sigma}_y^{l+1}) + \Delta \hat{\sigma}_z^l \hat{\sigma}_z^{l+1}. \quad (33)$$

Thus, the average steady-state heat currents for the l th spin in the upper (lower) branch become

$$I_{U(D)} = Tr(\hat{I}[l] \cdot \hat{\rho}_S), \quad (34)$$

Average current flowing out of a bath is derived from the Liouville operator and is given as [2,7]

$$\langle I_L \rangle = Tr[\mathcal{L}_L \hat{\rho}_S \hat{H}_S]. \quad (35)$$

Magnetization of the system is defined with respect to the $\hat{\sigma}_z$ operator of each spin. To avoid confusion, we will use the notation $N_s(N_E \uparrow, N_G \downarrow)$, where N_s is the total number of spins, $N_E(N_G)$ is the number of spins in excited (ground) eigenstate. The average magnetization of a spin i is defined as

$$M_i = Tr(\hat{\sigma}_i^z \cdot \hat{\rho}_S). \quad (36)$$

The spin-spin correlation along the z direction is given as

$$\langle \hat{\sigma}_i^z \hat{\sigma}_j^z \rangle = Tr(\hat{\sigma}_i^z \hat{\sigma}_j^z \cdot \hat{\rho}_S). \quad (37)$$

We also use the concurrence [62] as a measure of entanglement between two spins; it is given by the following formula:

$$C(\hat{\rho}) = \max[0, \lambda_1 - \lambda_2 - \lambda_3 - \lambda_4], \quad (38)$$

where λ 's are the eigenvalues in decreasing order of the matrix $\hat{R} = \sqrt{\sqrt{\hat{\rho}} \hat{\rho} \sqrt{\hat{\rho}}}$ and $\hat{\rho}$ is the reduced density matrix for the two spin subsystems of interest with $\tilde{\rho} = (\hat{\sigma}_y \otimes \hat{\sigma}_y) \hat{\rho}^* (\hat{\sigma}_y \otimes \hat{\sigma}_y)$ and $\hat{\sigma}_y$ being the usual Pauli Y matrix. We will discuss in detail how the CM influences the correlations between the spins and the concurrence later.

Finally, we introduce the concept of ergotropy [63], which is defined as the maximum amount of work extractable from a quantum state under unitary time evolution. The state which is attainable by the unitary transformation and through which no work is extractable is called the passive state (for example, an equilibrium state). To find it, we first need to write the spectral decomposition of the steady-state density matrix as well as the system Hamiltonian in the following manner:

$$\begin{aligned} \hat{\rho}_S &= \sum_i r_i |\rho_i\rangle \langle \rho_i|, \quad \text{with } r_i \geq r_{i+1}, \\ \hat{H}_S &= \sum_i E_i |E_i\rangle \langle E_i|, \quad \text{with } E_i \leq E_{i+1}, \end{aligned} \quad (39)$$

where r_i, E_i and $|\rho_i\rangle, |E_i\rangle$ are the eigenvalues and corresponding eigenvectors of the density matrix and the system Hamiltonian, respectively. Given the above decompositions, the passive state ($\hat{\rho}_{\text{passive}}$) is defined as [31,63]

$$\hat{\rho}_{\text{passive}} = \sum_i r_i |E_i\rangle \langle E_i|. \quad (40)$$

The ergotropy (ϵ) is then defined as

$$\begin{aligned} \epsilon &= \text{Tr}(\hat{H}_S \cdot \hat{\rho}_S) - \text{Tr}(\hat{H}_S \cdot \hat{\rho}_{\text{passive}}) \\ &= \sum_{i,j} r_i E_j (|\langle \rho_i | E_j \rangle|^2 - \delta_{i,j}). \end{aligned} \quad (41)$$

From the above discussion, we can infer that ergotropy can be used to quantify how far a system is from the passive state.

D. Information about numerical methodology

For solving the master equation given in Eq. (26), we again write it in the matrix form, though we use the more effective numerical method for the Redfield master equation defined in Ref. [55]. Numerically solving this equation by replacing the time derivative terms with 0 and imposing the constraint of fixed initial magnetization then gives us the steady-state density matrix [57]. Once we have the steady-state density matrix, all the quantities of interest can be evaluated from the definitions given in Sec. III C. It is important to note that the Redfield master equation is not guaranteed to be trace preserving and totally positive [59], so we also check if the obtained solutions have negative probabilities. For the parameter range we work on, no such regions were found. We now discuss in detail the results for the quantum model below.

E. Results

As seen in Fig. 10, large CM can be achieved just by having an unequal number of spins in the branches if the total magnetization is conserved and the asymmetry parameter Δ is in the suitable range. In Fig. 10(a), on plotting the currents with the asymmetry parameter Δ for the five-spin setup $5(3\uparrow 2\downarrow)$, we see that CM occurs for positive values of asymmetric interaction parameter Δ . We also see that the onset of CM is marked by a sudden dip in the total current near $\Delta \sim 0$. Interestingly, on reversing the magnetization via a configuration change $5(3\uparrow 2\downarrow) \rightarrow 5(2\uparrow 3\downarrow)$, the total current remains the same and CM also occurs for a certain parameter range but the branch currents drastically change, as seen in Fig. 10(b).

In Fig. 10(c), we observe that the dip in the total current is sharper for a six-spin system and is accompanied by CM in a narrow range. Finally, on plotting the currents with the temperature of the left bath T_L while keeping the temperature of right bath T_R fixed in Fig. 10(d), we see that the magnitude of currents initially increase nonmonotonically with an increase in the value of T_L , but they plateau for larger temperature differences. On the other hand, the corresponding CM initially increases for a small region, reaches a maximum, and then starts decreasing before finally vanishing at some finite temperature difference. We also look at the spin-spin correlation along the z direction and concurrence between

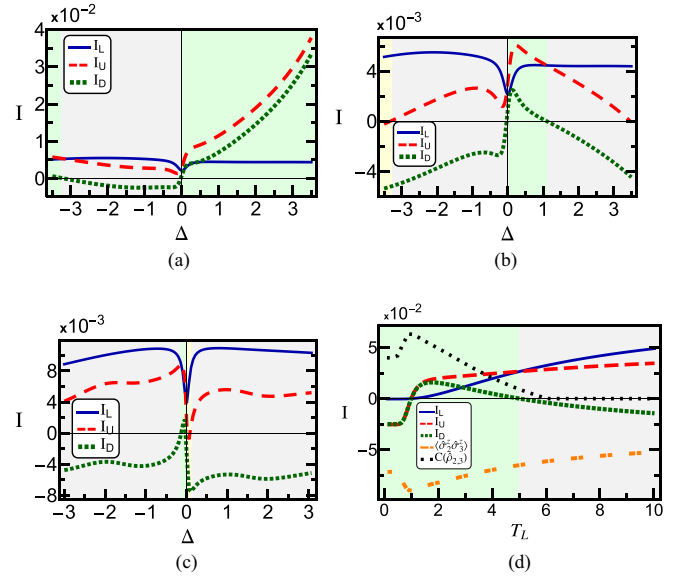


FIG. 10. Variation of heat currents (I) with the asymmetry parameter Δ for (a) setup $5(3\uparrow 2\downarrow)$, (b) setup $5(2\uparrow 3\downarrow)$, (c) a six-spin system with setup $6(4\uparrow 2\downarrow)$ with $N_U = 3, N_D = 1$, and (d) variation of heat currents (I), correlation, and concurrence between spins 2 and 3 with T_L for $\Delta = 2.1$. For all cases unless otherwise specified, we work with the setup $5(3\uparrow 2\downarrow)$ and $T_L = 2, T_R = 1, J = 1$. In (d), we scale the correlation and concurrence by a factor of 0.2 for the visual convenience.

spins 2 and 3 in Fig. 10(d) to check the dependence of CM on correlations. We see that similar to the CM, correlation and concurrence initially increase for a small region and then start declining with an increase in temperature of the left bath. Concurrence shows a sharper decline as compared to the spin-spin correlation. Note that $\langle \hat{\sigma}_2^z \hat{\sigma}_3^z \rangle$ is negative because of the antiferromagnetic interaction between the spins. We try to understand the above observations in the following discussion.

We discuss only the five-spin setup $5(3\uparrow 2\downarrow)$. The results in Fig. 10 above showed that the onset of current circulation is accompanied by a dip in total current near $\Delta \sim 0$. To understand why the total current drops, we study the properties of the occupied energy levels. It turns out that the nonzero occupancy is seen in only ten energy levels. These levels correspond to ten different configurations having the same magnetization. Out of these, only six energy levels are nondegenerate, numbering these energy levels in ascending order of their energies we plot $E_1, E_2, E_3, E_4, E_5, E_6$ with Δ in Fig. 11(a) and observe that the energy levels E_4 and E_5 intersect each other at $\Delta = 0$. The other energy levels are sufficiently far from each other in the plotted region. This means that the system loses one phonon transfer channel through which heat current can pass at $\Delta = 0$ and, as a result, the total heat current decreases. To check what happens to the probability of occupancy corresponding to these energy levels, we plot the variation of probability of occupancy with Δ for the same range in Fig. 11(b). We see that P_2 suddenly drops and P_3 increases, indicating population inversion be-

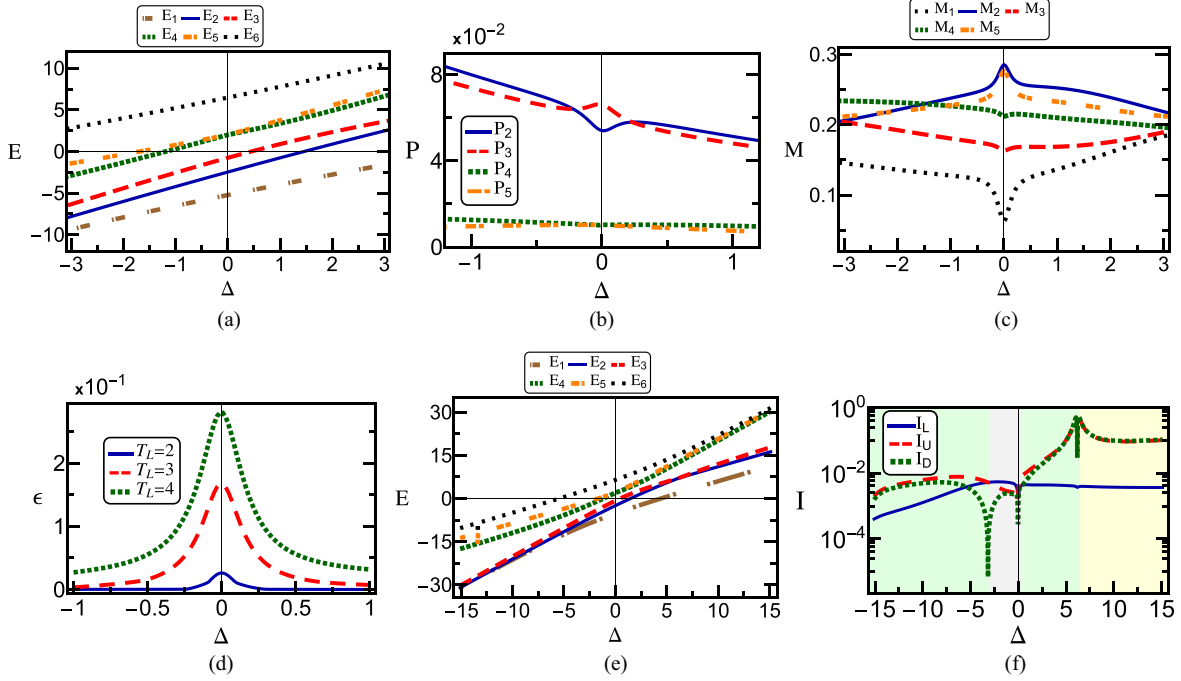


FIG. 11. (a) Variation of energy levels with Δ , (b) variation of occupation probability (P) with Δ , (c) variation of individual spin magnetization (M_i) with Δ , (d) variation of ergotropy (ϵ) with Δ , variation of (e) energy levels and (f) currents for a larger range of asymmetry parameter Δ . Note that only the magnitude of currents are considered for the log plot in (f) but the background colors for parallel, clockwise, or anticlockwise circulating currents are kept. For all cases unless otherwise specified, we work with the setup $5(3\uparrow 2\downarrow)$ and $T_L = 2$, $T_R = 1$, $J = 1$.

tween energy levels E_2 and E_3 near $\Delta = 0$. The probability of occupancy for other energy levels behaves in the expected way with higher energy levels having lesser probability of occupancy and vice versa. This can only happen if the system is far from the passive state defined in (40) and seems to suggest that the additional degeneracy in the two energy levels and the constraint of fixed initial magnetization is forcing the system to settle at states that are unfavorable, according to a passive state. We also plot the variation of individual spin magnetization with Δ in Fig. 11(c) and see that though the total magnetization remains fixed throughout this region, individual spin magnetization behaves in an atypical manner near $\Delta \sim 0$ with local minima or maxima dipping for each spin. To support our observations further, we evaluate the ergotropy as given in Eq. (41) but only consider the energy levels with nonzero probability of occupancy. Plotting the variation of ergotropy with Δ in Fig. 11(d), we see that the ergotropy suddenly starts rising around $\Delta \sim 0$, indicating the system does move farther away from the passive state in this region. Also, on increasing the temperature of the left bath, the ergotropy increases as the system moves even further away from the passive state due to the increase in the temperature gradient.

All the above results seem to suggest that whenever two energy levels intersect, the physical observables of our system behave in an atypical manner. Even for a larger range of the asymmetric parameter $\Delta \in [-15, 15]$, very similar features are seen in energy levels and currents as shown in Figs. 11(e) and 11(f). This shows that whenever nondegenerate energy levels come close to each other, a transition from parallel to circulating currents can occur in the system. Though the above

discussion does help us to predict suitable conditions for current circulation, namely, ergodic constraints and additional degeneracies, we note that analyzing the phonon transfer mechanism between different energy levels might help us to get better insights into CM in quantum systems, but this is beyond the scope of the present paper [2,7].

IV. CONCLUSION

To conclude, we study heat CM due to branch spin number asymmetry in classical and quantum spin systems. We find that CM is absent in the classical Q2R model for symmetric branch interaction strengths. We then employ different spin-spin interaction strengths in the upper and lower branches and show that this inequality is enough to generate as well as manipulate the CM. This happens even if we have the same number of spins in both branches. We then provide a possible physical mechanism responsible for CM in such systems. Similar features and heat current values are found if we use the CCA model instead of the Q2R model. This shows that the presence of additional momentum energy in the system does not contribute appreciably to the steady state currents. This is in accordance with earlier studies with such dynamics. We then study a five spin quantum system with modified Heisenberg XXZ interaction and preserved magnetization using the Redfield master equation. We, with detailed numerical analysis, show that it is possible to generate CM just by the branch spin number asymmetry in this model for a suitable range of asymmetry parameter Δ . Our results indicate that the onset of CM is accompanied by a sudden dip in total current, which may be triggered due to the intersection of two energy

levels for certain values of Δ . It is seen that this value of Δ also corresponds to population inversion and atypical trends for other physical observables, e.g., magnetization. Since the two factors, namely, the ergodic constraint due to fixed magnetization and additional degeneracies in the system push the system away from the passive state, we deduce that they may be the main causes for CM. This deduction is also supported by the ergotropy evaluations for our system. It is also seen that the total current is immune to the inversion of individual magnetization of the spins while the branch currents are not. We also find that for both the classical and quantum models, CM is only observed when temperature gradient and intrasystem interaction strength have similar orders of energy. This also points to the importance of correlation between spins required

for CM. In further studies, the relation of CM with ergodicity can be studied as both the classical and quantum systems considered here have nonergodic dynamics [44,46], and the effect of different spectral densities can also be explored in the quantum case.

ACKNOWLEDGMENTS

R.M. gratefully acknowledges financial support from the Science and Engineering Research Board (SERB), India, under the Core Research Grant (Project No. CRG/2020/000620). We also thank Özgür E. Müstecaplıoğlu and M. Tahir Naseem of the Koç University, Istanbul, for useful discussions and insights about this project.

-
- [1] S. Kaushik, S. Kaushik, and R. Marathe, *Eur. Phys. J. B* **91**, 87 (2018).
- [2] V. Upadhyay, M. T. Naseem, R. Marathe, and O. E. Müstecaplıoğlu, *Phys. Rev. E* **104**, 054137 (2021).
- [3] G. T. Landi, E. Novais, M. J. de Oliveira, and D. Karevski, *Phys. Rev. E* **90**, 042142 (2014).
- [4] J. W. Jiang, J. S. Wang, and B. Li, *Europhys. Lett.* **89**, 46005 (2010).
- [5] J. Ordonez-Miranda, Y. Ezzahri, and K. Joulain, *Phys. Rev. E* **95**, 022128 (2017).
- [6] D. Segal and A. Nitzan, *Phys. Rev. Lett.* **94**, 034301 (2005).
- [7] C. Kargı, M. T. Naseem, T. c. v. Opatrný, O. E. Müstecaplıoğlu, and G. Kurizki, *Phys. Rev. E* **99**, 042121 (2019).
- [8] D. Segal, *Phys. Rev. Lett.* **100**, 105901 (2008).
- [9] L. Zhang, J. Thingna, D. He, J.-S. Wang, and B. Li, *Europhys. Lett.* **103**, 64002 (2013).
- [10] M. Terraneo, M. Peyrard, and G. Casati, *Phys. Rev. Lett.* **88**, 094302 (2002).
- [11] O.-P. Saira, M. Meschke, F. Giazotto, A. M. Savin, M. Möttönen, and J. P. Pekola, *Phys. Rev. Lett.* **99**, 027203 (2007).
- [12] W. Chung Lo, L. Wang, and B. Li, *J. Phys. Soc. Jpn.* **77**, 054402 (2008).
- [13] Q. Ruan and L. Wang, *Phys. Rev. Res.* **2**, 023087 (2020).
- [14] M. T. Naseem, A. Misra, O. E. Müstecaplıoğlu, and G. Kurizki, *Phys. Rev. Res.* **2**, 033285 (2020).
- [15] J.-H. Jiang, M. Kulkarni, D. Segal, and Y. Imry, *Phys. Rev. B* **92**, 045309 (2015).
- [16] Y. Zhang, Z. Yang, X. Zhang, B. Lin, G. Lin, and J. Chen, *Europhys. Lett.* **122**, 17002 (2018).
- [17] R. Sánchez, H. Thierschmann, and L. W. Molenkamp, *Phys. Rev. B* **95**, 241401(R) (2017).
- [18] R. Messina, M. Antezza, and P. Ben-Abdallah, *Phys. Rev. Lett.* **109**, 244302 (2012).
- [19] J. Hwang, M. Pototschnig, R. Lettow, G. Zumofen, A. Renn, S. Götzinger, and V. Sandoghdar, *Nature (London)* **460**, 76 (2009).
- [20] A. Dhar, *Adv. Phys.* **57**, 457 (2008).
- [21] K. Poulsen, A. C. Santos, L. B. Kristensen, and N. T. Zinner, *Phys. Rev. A* **105**, 052605 (2022).
- [22] K. Poulsen, A. C. Santos, and N. T. Zinner, *Phys. Rev. Lett.* **128**, 240401 (2022).
- [23] A. Chioquetta, E. Pereira, G. T. Landi, and R. C. Drumond, *Phys. Rev. E* **103**, 032108 (2021).
- [24] B. Li, L. Wang, and G. Casati, *Phys. Rev. Lett.* **93**, 184301 (2004).
- [25] S. Y. Cho and R. H. McKenzie, *Phys. Rev. B* **71**, 045317 (2005).
- [26] S. Lepri, R. Livi, and A. Politi, *Phys. Rep.* **377**, 1 (2003).
- [27] N. Li, J. Ren, L. Wang, G. Zhang, P. Hänggi, and B. Li, *Rev. Mod. Phys.* **84**, 1045 (2012).
- [28] E. Pereira, *Phys. Rev. E* **96**, 012114 (2017).
- [29] R. Kosloff, *Entropy* **15**, 2100 (2013).
- [30] H. Kirchberg and A. Nitzan, *J. Chem. Phys.* **156**, 094306 (2022).
- [31] X. Xu, K. Choo, V. Balachandran, and D. Poletti, *Entropy* **21**, 228 (2019).
- [32] P. Dugar and C.-C. Chien, *Phys. Rev. E* **105**, 064111 (2022).
- [33] D. Roy, *J. Phys.: Condens. Matter* **20**, 025206 (2008).
- [34] D. Rai, O. Hod, and A. Nitzan, *J. Phys. Chem. C* **114**, 20583 (2010).
- [35] R. Marathe, A. Dhar, and A. M. Jayannavar, *Phys. Rev. E* **82**, 031117 (2010).
- [36] S. Bandopadhyay, P. S. Deo, and A. M. Jayannavar, *Phys. Rev. B* **70**, 075315 (2004).
- [37] A. Jayannavar, P. Singha Deo, and T. Pareek, *Phys. B: Condens. Matter* **212**, 261 (1995).
- [38] S. Xiao, X. Yang, L. Cai, and T. C. Liu, *Eur. Phys. J. B* **86**, 77 (2013).
- [39] S. Nakanishi and M. Tsukada, *Phys. Rev. Lett.* **87**, 126801 (2001).
- [40] J. P. Eckmann and E. Zabey, *J. Stat. Phys.* **114**, 515 (2004).
- [41] A. M. Jayannavar and P. Singha Deo, *Phys. Rev. B* **51**, 10175 (1995).
- [42] G. Y. Vichniac, *Physica D* **10**, 96 (1984).
- [43] K. Saito, S. Takesue, and S. Miyashita, *Phys. Rev. E* **59**, 2783 (1999).
- [44] M. Creutz, *Ann. Phys.* **167**, 62 (1986).
- [45] M. Schulte, W. Stiefelhagen, and E. S. Demme, *J. Phys. A: Math. Gen.* **20**, L1023 (1987).
- [46] D. Stauffer, *Comput. Phys. Commun.* **127**, 113 (2000).
- [47] R. Coldea, D. A. Tennant, E. M. Wheeler, E. Wawrzynska, D. Prabhakaran, M. Telling, K. Habicht, P. Smeibidl, and K. Kiefer, *Science* **327**, 177 (2010).
- [48] W. P. Wolf, *Braz. J. Phys.* **30**, 794 (2000).

- [49] K. Micadei, J. P. S. Peterson, A. M. Souza, R. S. Sarthour, I. S. Oliveira, G. T. Landi, T. B. Batalhão, R. M. Serra, and E. Lutz, *Nat. Commun.* **10**, 2456 (2019).
- [50] J. Zhang, F. M. Cucchiatti, C. M. Chandrashekar, M. Laforest, C. A. Ryan, M. Ditty, A. Hubbard, J. K. Gamble, and R. Laflamme, *Phys. Rev. A* **79**, 012305 (2009).
- [51] M. Seo, H. K. Choi, S.-Y. Lee, N. Kim, Y. Chung, H.-S. Sim, V. Umansky, and D. Mahalu, *Phys. Rev. Lett.* **110**, 046803 (2013).
- [52] M. C. Rogge and R. J. Haug, *Phys. Rev. B* **77**, 193306 (2008).
- [53] A. Bermudez, M. Bruderer, and M. B. Plenio, *Phys. Rev. Lett.* **111**, 040601 (2013).
- [54] D. Porras and J. I. Cirac, *Phys. Rev. Lett.* **92**, 207901 (2004).
- [55] W. T. Pollard and R. A. Friesner, *J. Chem. Phys.* **100**, 5054 (1994).
- [56] S. Wolfram, *Rev. Mod. Phys.* **55**, 601 (1983).
- [57] A. W. Sandvik, *AIP Conf. Proc.* **1297**, 135 (2010).
- [58] P. Coleman, Simple examples of second quantization, in *Introduction to Many-Body Physics* (Cambridge University Press, Cambridge, 2015), p. 7194.
- [59] H. P. Breuer and F. Petruccione, *The Theory of Open Quantum Systems* (Oxford University Press, Oxford, 2002).
- [60] M. Cattaneo, G. L. Giorgi, S. Maniscalco, and R. Zambrini, *New J. Phys.* **21**, 113045 (2019).
- [61] D. Tupkary, A. Dhar, M. Kulkarni, and A. Purkayastha, *Phys. Rev. A* **105**, 032208 (2022).
- [62] W. K. Wootters, *Phys. Rev. Lett.* **80**, 2245 (1998).
- [63] A. E. Allahverdyan, R. Balian, and T. M. Nieuwenhuizen, *Europhys. Lett.* **67**, 565 (2004).